Colloid & Polymer Science Colloid Polym Sci 272: 1175–1189 (1994)

Leading Contribution

Colloidal stability of calcite dispersion treated with sodium polyacrylate

K. R. Rogan, A. C. Bentham, I. A. George, and D. R. Skuse

Research Department, ECC International.

Abstract: The stabilising action of sodium polyacrylate on colloidal dispersions of calcite has been investigated through measurement of viscosity, ion concentration and electrophoretic mobility. The dose of sodium polyacrylate was in the range 0 to 28 mg per g of calcite and the dispersions were prepared at a solids content of 70% (by weight). The ionic strength of the dispersions, ca. 0.005 to 0.5, increased with dose. An increase in divalent ion concentration with dose was attributed to sodium polyacrylate-ion exchange.

The stabilising action of sodium polyacrylate was evident from the sharp fall in viscosity observed at low levels of addition, and the invariance of this low viscosity throughout the remainder of the dose range. The stability of the dispersions at low doses was quantified by DLVO theory and attributed to electric double layer (EDL) repulsion. However, at higher doses, and with the resultant EDL compression, DLVO theory was found inadequate. Instead, recourse was made to steric stabilisation theories in order to explain the observed stability. A model was formulated to characterise the observed multilayer uptake of polyacrylate at higher doses. The steric repulsion evaluated using this model increased with dose and explained the observed higher dose stability. The stability over the dose ranges < 2, 2 to 6, and > 6 mg per g is best described as arising from, respectively, electrostatic, electrosteric and steric repulsions.

Key words: Sodium-polyacrylate – calcite-dispersion – colloidal-stability – slurry-viscosity – paper

Introduction

Since the production of low viscosity, colloidally stable calcite slurry at a high solids content necessitates the addition of sodium polyacrylate (NaPolyA), it is essential to understand both qualitatively and quantitatively the fundamental processes, involving both the mineral and the dispersant, which give rise to this stability.

Aqueous slurries of finely ground calcite find a wide range of applications in the paper industry. The ideal slurry is at a high solids content in order to minimise transportation and storage costs, and has a low viscosity to facilitate processing. In order to prepare such a slurry it is necessary to add a dispersant to reduce the viscosity. The industry standard dispersant for this application is NaPolyA.

In a broader context, a study of the calcite/NaPolyA system will provide a fundamental understanding of the polyelectrolyte stabilisation of colloids.

Materials

The dispersed phase

Fine calcite was prepared from Carrara marble by low solids, dispersant-free grinding and subsequent filtration. The resultant carbonate (99% calcite, by chemical analysis) was in the form of a high-solids content (ca. 76%) plug, which was subsequently sliced/broken down into a more manageable form.

The weight-averaged size distribution of the calcite particles was recorded on a Micromeritics

Sedigraph; the particles were assumed to be spheres. The weight-averaged median radius of the particles was calculated to be 515 ± 10 nm. The amount of material smaller than 1 μm radius was ca. 90%. The weight-based distribution was translated into a number-averaged size distribution by the Micromeritics software. The number-averaged, median radius of the particles (R, in units of nm) was calculated to be 193 ± 23 nm. From R, the geometric specific surface area (S, in units of $m^2 g^{-1}$) of the particles was calculated using the expression

$$S = 3 \times 10^9/(p_1 r) , \quad (1)$$

where p_1 is the density of calcite (2.71×10^6 g m^{-3}), and $r = R$. The value of 5.7 $m^2 g^{-1}$ was obtained for S, which was not significantly different from the measured N_2 BET area of 6.3 ± 1.0 $m^2 g^{-1}$.

A polyacrylate-free suspension of the calcite in distilled water was pressure filtered at 4.14 N m^{-2} on a multi-filament woven fabric for 45 min. The supernatant was clarified by further pressure filtration at ca. 0.48 to 0.62 N m^{-2} (with N_2) through a 0.1 μm cellulose nitrate membrane. The resultant solution was analysed for the more common elements found in aqueous environments[1], by inductively coupled plasma atomic emission spectroscopy (ICP). This revealed the presence of Ca, Na and Mg, and trace amounts of K. The Mg originates from small amounts (< 1%) of dolomite that are invariably found in Carrara marble.

The dispersing agent.

The NaPolyA was the sodium salt of a linear homopolymer of polyacrylic acid. It was obtained as a high concentration solution from Allied Colloids. The potentiometric titration of this solution against NaOH gave a weight/weight percent NaPolyA concentration (A) of 39.1 ± 0.5%, a weight/weight percent degree of Na^+-neutralisation of 99.2 ± 0.2% and a Na^+ concentration of 4.168 mol kg^{-1}. The solution was analysed for the more common elements found in aqueous environments by ICP. This revealed, in addition to the expected high level of Na, a measurable level of S (probably in the form of the end group ϕOSO_3^-) and trace amounts of K. The high concentration solution was diluted with distilled water to give 1000 g of a dilute stock solution with an A of 12.8% and a Na^+ concentration of 1.365 mol kg^{-1}.

The molecular weight (M) of the polymer was that preferred for the dispersion of calcite, and was in the range 3500 to 9500 g mol^{-1} (as determined by low-angle laser light scattering).

Apparatus

Gel permeation chromatography (GPC) mobile phase was 0.025 mol dm^{-3} $NaH_2PO_4 2H_2O$ and Na_2HPO_4, 0.1 mol dm^{-3} NaCl and 0.02 weight/volume % NaN_3 in distilled water. The pH of the mobile phase was 6.8 ± 0.2 and it was filtered (0.2 μm cellulose acetate membrane) and degassed (vacuum and ultrasonication) prior to use. A blanket of He was maintained over the mobile phase. The GPC stationary phase was a Polymer Laboratories 300×7.5 mm aquagel-OH 40 column (protected by a guard column). Operational Settings of the GPC system: a) Pump flow rate 16.7 mm^3 s^{-1}; b) Sample loop size 20 mm^3; c) UV detector wavelength 222 nm; d) Data collection by Jones Chromatography JCL6000 GPC software.

Method

Contacting of dispersed phase and dispersing agent

The dispersed phase and the dispersing agent were contacted at a solids content of 70% (volume fraction (ϕ) = 0.463) for about 2 days as follows. Fine calcite, equivalent to a dry weight of 140 g, was weighed into a brass mixing pot. A known weight of NaPolyA was added, in the form of the dilute stock solution, such that the weight of NaPolyA per unit weight of calcite (i.e. the NaPolyA dose) was in the range 0 to 28 mg per g calcite. Finally, sufficient water was added such that the total weight of the contents of the pot was 200 g. The contents of the pot were homogenised initially by hand and then using a mechanical mixer.

[1] Na, S, Si, Ca, Mg, K, Al, P, Fe, B, Zn and Cu

Slurry viscosity measurement and slurry separation

The initial viscosity of the slurry was measured using a Brookfield viscometer (model RV) at 1.67 revs. s^{-1}. About 2 cm^3 of the slurry was retained while the remainder was separated into solid and supernatant phases by pressure filtration (as described above).

Analysis of supernatant

A part of the supernatant was analysed for the elements Na, Ca, S and Mg by ICP. In addition, a part of the supernatant was analysed for cation polyacrylate (CATPA) by GPC. The remainder of the supernatant was retained for electrophoretic mobility measurements.

Electrophoretic mobility measurements

An appropriately small amount of the slurry was redispersed in the supernatant and the electrophoretic mobility of the suspended particles measured using a Malvern Zetasizer-4 instrument.

Repetition

This entire procedure was repeated 23 times. With each repeat the dose administered to the calcite was a value in the range 0 to 28 mg per g calcite, such that the dosage difference between repeats was roughly 0.5 mg per g at low doses (i.e. < 10 mg per g) and roughly 5 mg per g at higher doses.

Results and discussion

Viscosity

The initial Brookfield viscosity data of the twenty-four slurries are presented as a plot of viscosity against dose in Fig. 1. The sharp fall in viscosity at low levels of addition, and the invariance of this low viscosity throughout the remainder of the dose range demonstrated the stabilising action of NaPolyA on colloidal dispersions of calcite.

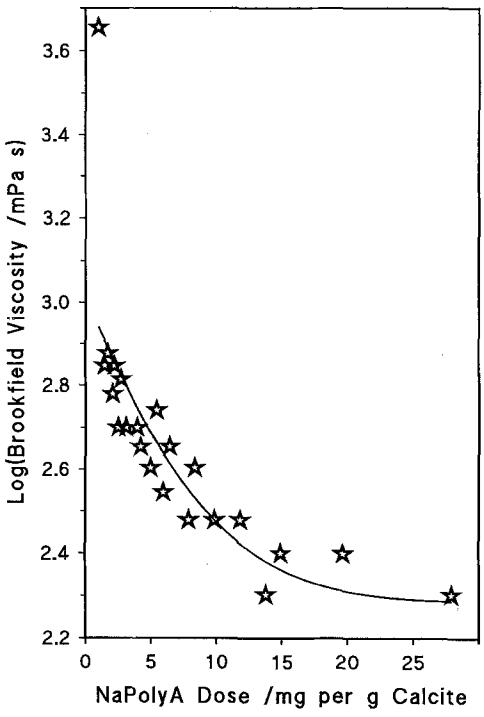

Fig. 1. Brookfield viscosity as a function of NaPolyA dose.

Solution species

The principal species found in each supernatant were Na^+, CATPA, Ca^{2+}, ϕOSO_3^- and Mg^{2+}. The quantitative analyses of Na^+ and Ca^{2+} are presented as plots of solution concentration against dose in Fig. 2.

The pH of the supernatants was in the range ca. 9.2 to 9.5, except for the supernatant obtained from the lowest-dosed (i.e. 0.49 mg per g) slurry which had a pH of 8.4; the undosed slurry supernatant had a pH of 6.4.

In general, above a dose of ca. 1.0 mg per g the solution concentrations of all the principal species increased with dose. In the case of Na^+, CATPA and ϕOSO_3^- this increase was linear, whereas the concentrations of Ca^{2+} and Mg^{2+} tended towards limiting values at high levels of addition. At dose levels of ≤ 1.0 mg per g, however, the concentration behaviour of the various species was not uniform. Thus, no CATPA was found in solution, while the concentration of Ca^{2+} and Mg^{2+} decreased with increasing dose. In contrast, the concentration of Na^+ increased linearly, with an intercept close to the origin. The ϕOSO_3^- concentration increased rapidly up to 1.0 mg per g

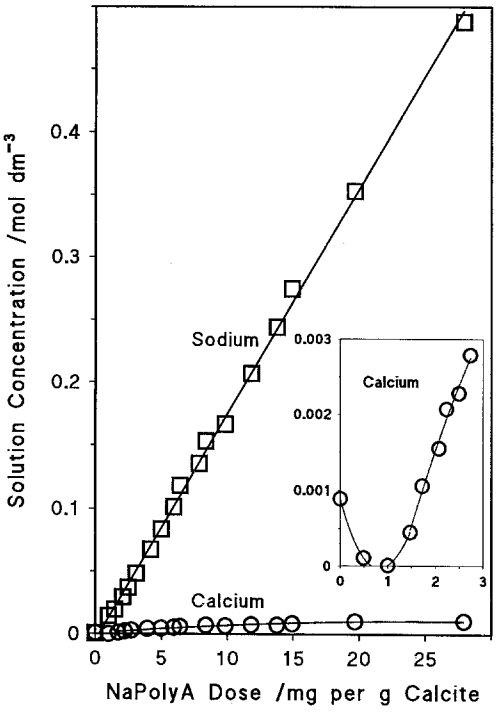

Fig. 2. Sodium and calcium solution concentrations as functions of NaPolyA dose

and thereafter increased at a slower rate with increasing dose.

The behaviour of Ca^{2+} and Mg^{2+} concentrations at very low doses (i.e. ≤ 1.0 mg per g) may be explained in terms of an initial reaction of these alkaline earth cations with NaPolyA to produce mixed cation polyacrylates (eg. sodium-calcium-polyacrylate), followed by the uptake of these polyacrylates by the calcite. This explanation implies that the polyacrylate acted as an ion exchanger and exchanged Na^+ ions for Ca^{2+} and Mg^{2+} ions. From a thermodynamic point of view, such an exchange is predicted on the basis of the small solubility product values (ca. 10^{-6} to 10^{-20} $mol^2\,dm^{-6}$) of Ca^{2+} and Mg^{2+} carboxylates and the vast difference between these values and the much larger values of Na^+ carboxylates [1, 2].

In a similar way, the increasing concentrations of Ca^{2+} and Mg^{2+} with dose above 1.0 mg per g may also be explained in terms of a polyacrylate ion-exchange reaction. However, this time Na^+ ions of the polyacrylate are exchanged for Ca^{2+} and Mg^{2+} ions from the solid phase, and the so-formed water soluble, mixed cation polyacrylate now remains in the solution phase.

It is to be noted that the observed zero values of alkaline earth concentrations, at a dose of ca. 1.0 mg per g (see Fig. 2, for Ca^{2+}), is somewhat at variance with the obvious excess of calcite over polyacrylate in this system; an excess of calcite should have prohibited the fall of alkaline earth concentrations to zero values. It may be inferred, therefore, that the system was not at equilibrium when the concentrations were recorded. In addition, the increase in alkaline earth concentration with dose (above ca. 1.0 mg per g) may be attributed, in part, to the increase in the solubility of mixed cation polyacrylate with increase in ionic strength.

The calculation of the concentrations of polyacrylate repeating unit anions associated with Ca^{2+}, Mg^{2+} *and* Na^+ *ions*

In order to satisfy the condition of electroneutrality in the solution phase, associations were sought between oppositely charged ionic species. The associations involving polyacrylate repeating unit anions (PA^-) are discussed in this section, while associations involving Na^+ ions are discussed in the next section. Throughout all discussions, the mol dm^{-3} concentration of species i, of molecular weight m_i g mol^{-1}, is designated $[i]$ and the mg cm^{-3} concentration of species i is designated $\langle i \rangle$, such that

$$\langle i \rangle = m_i[i] \tag{2}$$

The concentrations (respectively, $[PA^-]_{Ca}$ and $[PA^-]_{Mg}$) of those PA^- ions associated with Ca^{2+} and Mg^{2+} ions (i.e. $CaPA_2$ and $MgPA_2$) were calculated from the measured (ICP) concentrations of Ca and Mg. Thus, $[PA^-]_{Ca} = 2[Ca^{2+}]$ and $[PA^-]_{Mg} = 2[Mg^{2+}]$.

The concentration ($[PA^-]_{Na}$) of those PA^- ions associated with Na^+ ions (i.e. NaPA) was calculated from the difference between the measured (GPC) concentration of CATPA and the sum of the concentrations of $CaPA_2$ and $MgPA_2$. Thus,

$$[PA^-]_{Na} = (\langle CATPA \rangle - (\langle CAPA_2 \rangle + \langle MgPA_2 \rangle))/m_{NaPA}\,, \tag{3}$$

where $\langle CaPA_2 \rangle$ and $\langle MgPA_2 \rangle$ were obtained from, respectively, $[Ca^{2+}]$ and $[Mg^{2+}]$ using Eq.

(2) with the appropriate value for m_i, i.e. either 182.2 g mol^{-1} ($CaPA_2$) or 166.4 g mol^{-1} ($MgPA_2$), and m_{NaPA} is the molecular weight of NaPA (94.05 g mol^{-1}).

The concentrations of NaPA ([NaPA]) and alkaline earth polyacrylate ([$CaPA_2$ + $MgPA_2$]) were similar at low doses (i.e. < 2 mg per g). However, at higher doses [NaPA] increased with dose at a much greater rate than did [$CaPA_2$ + $MgPA_2$], and by the highest dose [NaPA] was ca. 20 times greater than [$CaPA_2$ + $MgPA_2$] (i.e. ca. 0.470 mol dm^{-3} compared to ca. 0.024 mol dm^{-3}).

The calculation of the concentrations of Na^+ *ions associated with* PA^-, ϕOSO_3^- *and* HCO_3^- *ions*

The concentrations (respectively, $[Na^+]_{PA}$ and $[Na^+]_{\phi OSO_3}$) of those Na^+ ions associated with PA^- and ϕOSO_3^- (i.e. NaPA and $Na\phi OSO_3$) were given, respectively, by the equivalences $[Na^+]_{PA} = [PA^-]_{Na}$ and $[Na^+]_{\phi OSO_3} = [\phi OSO_3^-]$.

The concentration ($[Na^+]_{HCO_3}$) of those Na^+ ions associated with HCO_3^- ions (i.e. $NaHCO_3$) was calculated from the difference between the measured (ICP) concentration of Na ions and the sum of the concentrations $[Na^+]_{PA}$ and $[Na^+]_{\phi OSO_3}$. Thus,

$$[Na^+]_{HCO_3} = [Na^+] - ([Na^+]_{PA} + [Na^+]_{\phi OSO_3}) . \quad (4)$$

Throughout most of the dose range, $[NaHCO_3]$ was fairly steady at ca. 0.015 mol dm^{-3}, while $[Na\phi OSO_3]$ increased only slightly (ca. 0.002 to 0.008 mol dm^{-3}) with dose.

Ionic strength

The ionic strength (I) of each supernatant was calculated in the conventional way, from mol dm^{-3} ionic concentrations, using an expression of the form

$$I = 0.5(2^2[Ca^{2+}] + 1^2[PA^-]_{Ca} + 2^2[Mg^{2+}] + 1^2[PA^-]_{Mg} + 1^2[\phi OSO_3^-] + 1^2[Na^+]_{\phi OSO_3} + 1^2[Na^+]_{PA} + 1^2[PA^-]_{Na} + 1^2[Na^+]_{HCO_3} + 1^2[HCO_3^-]) , \quad (5)$$

where $[HCO_3^-]$ was given by the equivalence $[HCO_3^-] = [Na^+]_{HCO_3}$. Thus,

$$I = 0.5([Na^+] + [PA^-] + [\phi OSO_3^-] + [HCO_3^-]) + 2([Ca^{2+}] + [Mg^{2+}]) , \quad (6)$$

where

$$[PA^-] = [PA^-]_{Ca} + [PA^-]_{Mg} + [PA^-]_{Na} . \quad (7)$$

I increased linearly with dose, with an intercept close to the origin. The major contributors to I were Na^+ and PA^-. For example, at a dose of ca. 5.0 mg per g the I was 0.1004 of which 0.0418 was due to Na^+ and 0.0391 was due to PA^-; the minor contributors were Ca^{2+} (0.0090) and HCO_3^- (0.0067). Consequently, the form of the dose versus I plot is similar to the dose versus $[Na^+]$ plot shown in Fig. 2.

Electrical double layers of the particles

The increase in I across the dose range studied affected the electrical double layers (EDLS) of the particles. Thus, the effective thickness of the particle EDLS, as quantified by the reciprocal of the (I dependent) Debye–Huckel parameter (K), decreased by about an order of magnitude (ca. 5.3 to 0.4 nm). This was reflected in an increase in the ratio of particle radius to EDL thickness (KR) from $KR = 36$ to $KR = 457$.

The calculation of the quantities of abstracted species

The interaction of polyacrylate with calcite is better described as an abstraction rather than an adsorption process. This is because of the very likely occurrence of a chemical reaction between a portion (at least) of the interacting polyacrylate and the carbonate surface [3–6]. In this event, it is reasonable to assume that the polyacrylate/calcite system under study did not attain a state of equilibrium in the time scale of the experiment [7]. Thus, the concentration of CATPA found in solution (⟨CATPA⟩) was considered as a residual concentration, at the time of sampling, rather than an equilibrium concentration.

The total amount (γ_{TOT}, in units of mg per g Calcite) of CATPA abstracted was evaluated, for each dose, from the difference between the amount of NaPolyA administered to the calcite,

and ⟨CATPA⟩. This abstracted amount was converted into an abstraction density (Γ_{TOT}, in units of $\mu g\,m^{-2}$) using the geometric specific surface area of the calcite ($5.7\ m^2\,g^{-1}$).

An abstraction isotherm (Fig. 3) was constructed from a plot of Γ_{TOT} against ⟨CATPA⟩. This isotherm may be conveniently divided into three dose-range regions for the purposes of discussion (see Table 1). Over the first two regions, the isotherm has a rectangular hyperbolic shape with an initial sharp rise in abstraction in Region 1 followed by a short plateau in Region 2. This shape of isotherm obeys the Langmuir model, and the abstraction data can be fitted to the linear equation

$$\langle CATPA\rangle/\Gamma_{TOT} = K_L/(\Gamma_{TOT})_P + \langle CATPA\rangle/(\Gamma_{TOT})_P\,, \quad (8)$$

where K_L is a constant and $(\Gamma_{TOT})_P$ is the abstraction density at the plateau. Thus, a plot of $\langle CATPA\rangle/\Gamma_{TOT}$ against ⟨CATPA⟩ should yield a straight line having a slope of $1/(\Gamma_{TOT})_P$ from which the value of $(\Gamma_{TOT})_P$ may be readily obtained. Such a plot is shown in Fig. 4. There was a good correlation between $\langle CATPA\rangle/\Gamma_{TOT}$ and ⟨CATPA⟩ (correlation coefficient = 0.99) up to the end of Region 2. The value of $369.7\ \mu g\,m^{-2}$ was obtained for $(\Gamma_{TOT})_P$. The isotherm as a whole

Table 1. Division of abstraction data into three dose-range regions

Region	Dose range	⟨CATPA⟩ range
	mg per g Calcite	$mg\,cm^{-3}$
1	0 to 2.1	0 to 1.1
2	2.1 to 6.4	1.1 to 10.2
3	6.4 to 27.9	10.2 to 46.6

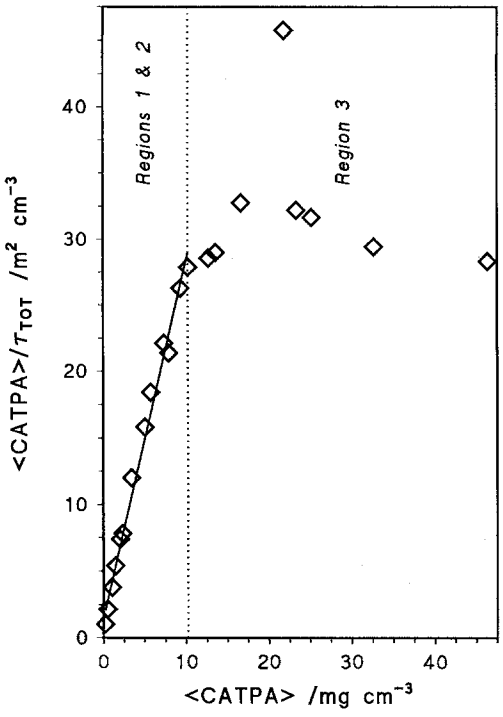

Fig. 4. Langmuir abstraction isotherm of cation polyacrylate on calcite

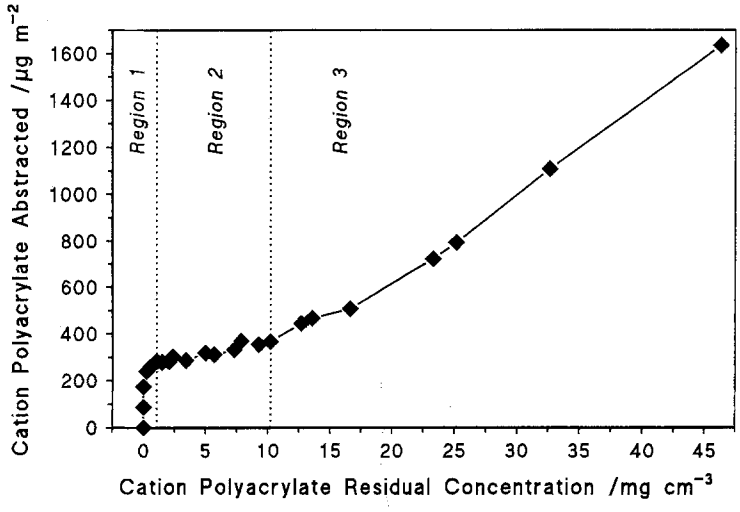

Fig. 3. Abstraction isotherm of cation polyacrylate on calcite

is of the type H3 in the Giles et al. [8] system of isotherm classification.

It may be inferred from the sharpness of the initial rise in abstraction (Region 1) that there was a high affinity of the polyacrylate molecules for the calcite surface [9], while the plateau at 369.7 $\mu g\,m^{-2}$ (Region 2) indicates the completion of an abstracted layer of polymer molecules. The shortness of the plateau means that the abstracted layer exposed a surface to the bulk solution which had nearly the same affinity for more polyacrylate as that of the original surface.

There was a small, but discernible, increase in Γ_{TOT} (ca. 84 $\mu g\,m^{-2}$) across the plateau region. This may be attributed to the development of the abstracted layer with increase in dose (i.e. increase in I). The increase in Γ_{TOT} with increase in I, across the plateau region, is shown in Fig. 5.

It is known that the excluded volumes of polyelectrolytes, such as polyacrylate, decrease appreciably with increase in I [10, 11]. This is because such an increase causes a shielding of charge centres which gives rise to a reduction in the long-range, electrostatic intra- and inter-molecular repulsions. The result is a collapse of polymer chains [12]. It would appear reasonable to assume, therefore, that the increase in I (ca. 0.036 to 0.139) across the plateau region brought about a collapse of the polyacrylate chains in the abstracted layer and the production of vacant sites on the calcite surface. Further polyacrylate was then able to bind to these vacant sites, thereby generating an increase in Γ_{TOT} across the plateau region.

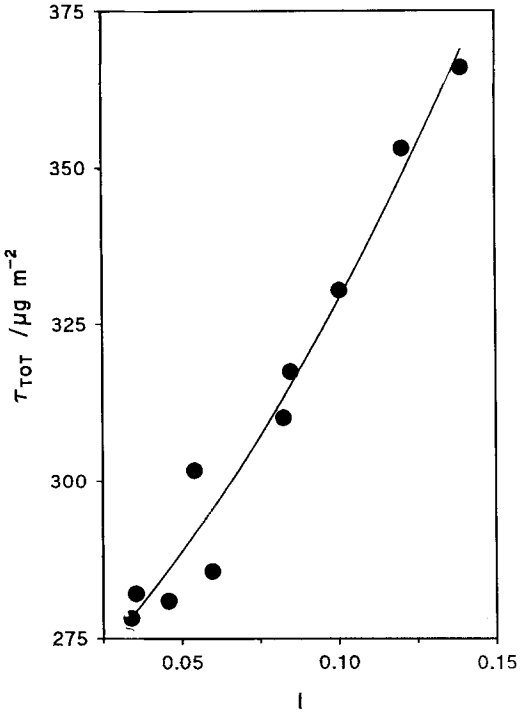

Fig. 5. Plateau abstraction density as a function of ionic strength (I)

Thus, the Γ_{TOT} value at the start of the plateau (ca. 282 $\mu g\,m^{-2}$) refers to a monolayer of extended polymer chains, while the Γ_{TOT} value at the end of the plateau (ca. 366 $\mu g\,m^{-2}$) refers to a monolayer of collapsed polymer chains.

In the third region of the isotherm there is a steady rise in abstraction, and no correlation was found between $\langle CATPA\rangle/\Gamma_{TOT}$ and $\langle CATPA\rangle$ (see Fig. 4). It may be inferred, therefore, that the further uptake of polyacrylate molecules occurred onto the layer of molecules initially abstracted, i.e., Region 3 describes multilayer formation. The reason for this multilayer formation may well lie with the increase in I (ca. 0.139 to 0.524) across Region 3. The effect of I on the amount of polyelectrolyte abstracted from solution has been studied by several groups [13, 14, 15, 16]. Irrespective of the relative signs of the surface charge and the polyelectrolyte, the abstracted amount generally increases with increasing I. Such behaviour arises from two sources: 1) the solvency of the solution for the polyelectrolyte decreases with increasing I, and 2) the shielding of the polyelectrolyte charge centres increases with I [12]. The combined effect of these two phenomena will be to drive the polyelectrolyte into the abstracted state.

Molecular footprint and molecular radius in the initial layer, up to the completion of this layer (i.e. Regions 1 and 2)

In the development of a layer, j, of abstracted polymer molecules (of average molecular weight $M\,g\,mol^{-1}$), the average molecular footprint (F_j, in units of nm^2) of a polymer chain on a surface may be obtained from the abstraction density attributable to that layer (Γ_j) by means of the relation

$$F_j = 10^{24} M/(\Gamma_j N)\,, \qquad (9)$$

where N is Avogadro's number. It is to be noted that Eq. (9) assumes that the collection of molecules taken up by a surface, at any stage in an abstraction processes, occupy all the available surface. Although this is a valid assumption when the collection of molecules form a complete monolayer, it is not strictly valid when the layer is incomplete, i.e. in the early stages of layer formation. However, in view of the high affinity isotherm observed for the abstraction process under study it is apparent that layers developed quickly over very narrow concentration ranges. Consequently, it was considered reasonable to apply Eq. (9) across the entire abstracted data range.

The average molecular footprint (F_1) of polyacrylate in the initial layer (i.e. $j = 1$) on calcite is given, therefore, by Eq. (9) with Γ_j set equal to the abstraction density (Γ_1) attributable to the initial layer. If it is assumed that F_1 is a circle, then the actual radius (r_{ABS}, in units of nm) of this circle is given by

$$r_{ABS} = (F/\pi)^{1/2} \tag{10}$$

with $F = F_1$, while the equivalent radius of gyration ($(r_G)_{ABS}$) is obtained using the expression

$$(r_G)_{ABS} = r_{ABS}/(5/3)^{1/2} \tag{11}$$

The appreciable variation in the excluded volumes, i.e. the radii of gyration, of polyelectrolytes with I was acknowledged earlier. The variation with I of the radius of gyration ($(r_G)_{SOL}$)) in bulk solution of NaPolyA, with a molecular weight in the range 3500 to 9500 g mol^{-1}, has been evaluated by Rogan [17] from the intrinsic viscosity data of Takahashi [18]. The variation is expressed as the second order polynomial

$$(r_G)_{SOL} = 2.3289 + 0.24166/I^{1/2} - 0.005175/I \tag{12}$$

It is reasonable to expect that $(r_G)_{ABS}$ will also vary with $1/I^{1/2}$, and in a similar fashion to that found for $(r_G)_{SOL}$. The variations of $(r_G)_{SOL}$ and $(r_G)_{ABS}$ with $1/I^{1/2}$ of the supernatants, are shown in Fig. 6; the values of $(r_G)_{ABS}$ were calculated from the abstraction data up to, and including, the development of the initial layer (i.e. up to the end of Region 2).

The collapsing effect of I on polyacrylate chains, whether in bulk solution or at a calcite surface, is evident from the general decrease in radii of gyration from ca. 4 to 2 nm with increasing I.

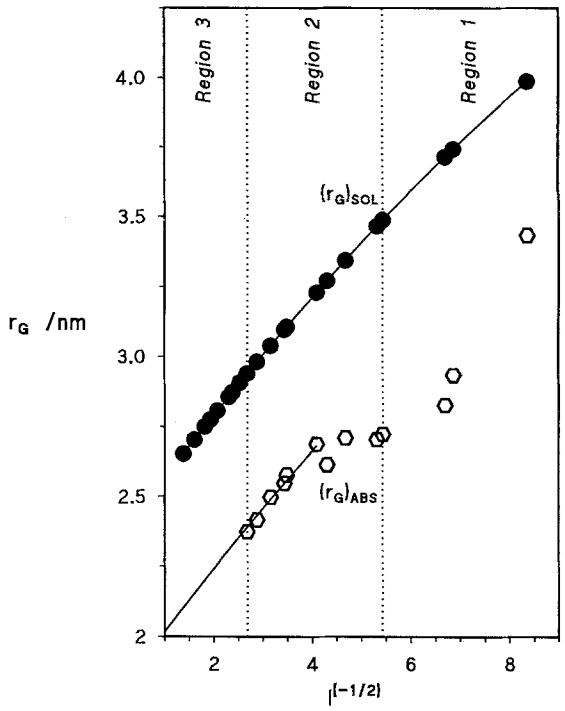

Fig. 6. Radii of gyration of solution ($(r_G)_{SOL}$) and abstracted ($(r_G)_{ABS}$) cation polyacrylate as functions of ionic strength (inverse square root)

On close inspection of Region 2 in Fig. 6 it is apparent that at high I the variation of $(r_G)_{ABS}$ with $1/I^{1/2}$ is very similar to that of $(r_G)_{SOL}$. Indeed, the difference between $(r_G)_{ABS}$ and $(r_G)_{SOL}$, at high I, has a steady value of ca. 0.549 nm, while the variation of $(r_G)_{ABS}$ with $1/I^{1/2}$ is described very well by an equation analogous to Eq. (12), viz.,

$$(r_G)_{ABS} = 1.7795 + 0.24166/I^{1/2} - 0.005175/I \tag{13}$$

This equation, therefore, describes the variation with I of the radius of gyration of polyacrylate chains in an abstracted monolayer. The curve of this equation is shown in Fig. 6.

Zeta potential

In view of the intermediate values of KR encountered in the present work, particularly at the

lower doses, the measured electrophoretic mobility was converted into zeta potential on the basis of the mathematical procedure developed by O'Brien and White [19], using the computer program containing this procedure written by White, Mangelsdorf and Chan [20].

The input into this program includes the concentrations, valencies and equivalent ionic conductivities at infinite dilution (Γ_0) of the principal ionic species present in the continuous phase surrounding the particles undergoing electrophoresis. In the case of two of the principal ionic species, viz., PA^- and ϕOSO_3^-, the Γ_0 values were taken to be those of simpler analogues. Thus, the PA^- ion was assigned the Γ_0 value of glutarate, while the ϕOSO_3^- ion was assigned the Γ_0 value of ethyl sulphate.

The zeta potential of the calcite particles is plotted as a function of dose in Fig. 7. Zeta potential increased with dose, reaching a maximum value of ca. − 50 mV at a dose of ca. 6 mg per g, i.e. just prior to multilayer formation. At higher doses, the zeta potential decreased with increasing dose. The initial rise in zeta potential is readily attributable to the uptake of polyacrylate (anionic polyelectrolyte) by the calcite surface (see Fig. 3). The fall in zeta potential at higher doses is reasonably explained in terms of the reduction in the decay distance of electrical potential incurred by the increase in I (see above). Apparently, this collapse of particle EDLS outweighs the increase in electrical potential expected with polyelectrolyte uptake.

Particle–particle interactions

Derjaguin and Landau [21] and Verwey and Overbeek [22] introduced the idea that colloid stability could be quantified on the basis of electrostatic repulsion and van der Waals attraction energies (V_R and V_A, respectively). That is, the potential energy of interaction (V_T) between approaching colloid particles is given by the sum ($V_R + V_A$). This idea has been applied in the present work, and the equations of Ottewill [23] and Verwey and Overbeek [22] were used to describe the variations of V_R and V_A, respectively, with inter-particle (surface to surface) distance (h, in

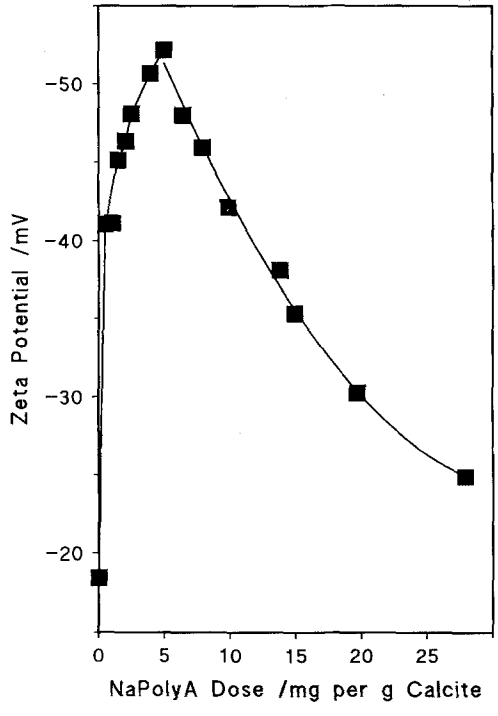

Fig. 7. Zeta potential as a function of NaPolyA dose

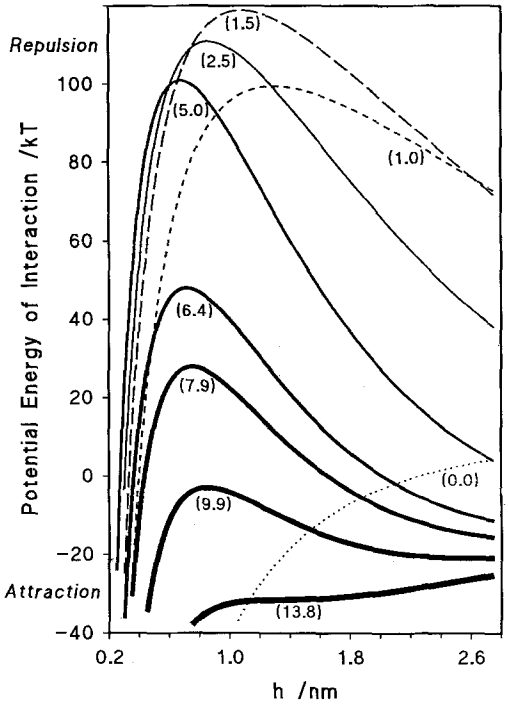

Fig. 8. Interaction energy curves: van der Waals attraction + electrostatic repulsion (no steric repulsive energy). Values in parentheses are NaPolyA dose in units of mg per g calcite

units of nm); the Hamaker constant was taken as 2.23×10^{-20} J [24].

The variation of V_T, scaled in units of kT, with h (interaction energy curve) is shown in Fig. 8, for a wide range of doses. The repulsive energy maxima of the interaction energy curves increase in height with increasing dose up to ca. 2 mg per g. Thereafter, the height of the energy maxima decrease with increasing dose. The increase at low dose is readily attributable to the increase in the zeta potential of these particles as they take up polyacrylate from low I solution.

At higher doses, the decrease in the height of the energy maxima may be attributed to the collapsing effect of I on EDLS, and the increasing importance of this effect at higher doses. Thus, although the zeta potential of the particles is observed to increase with dose above 2 mg per g, as polyacrylate is taken up, this is overshadowed by EDL collapse. The net effect is a loss of electrostatic repulsive energy and the energy maxima diminish with increasing dose.

Thus, on the basis of an inter-particle repulsion derived solely from electrostatics, the net potential energy of interaction between particles becomes less repulsive with increasing dose. That is, according to DLVO theory the colloidal stability of calcite slurry should diminish with dose above ca. 2 mg per g. However, this is at variance with the increase in colloid stability with dose inferred from the observed decay of slurry viscosity with dose, up to and beyond 6 mg per g. It would appear, therefore, that such stability cannot be explained solely on the basis of electrostatics, and that another repulsive energy exists between polyacrylate-covered calcite particles at high dose. It is highly likely that this energy is steric in origin. The remainder of this work describes the quantification of a steric repulsion energy, and its inclusion in the total potential energy of interaction between calcite particles.

A model of the polyacrylate abstracted by calcite in the region of multilayer formation

A necessary input into any steric energy term is the total thickness of the abstracted layer. In the present work, total layer thickness and other relevant parameters were evaluated using a model of polyacrylate uptake, based on polymer chain radii. A direct evaluation of layer thickness was not possible due to the polydispersity of both the calcite and the polyacrylate, and the expected relative thinness (in comparison with R) of such a low molecular weight polyacrylate layer.

Description of model

The model was formulated in such a way so as to be consistent with the observed behaviour of abstracted polyacrylate chains in the development of the initial layer: 1) After the completion of the initial layer, at a particular I, further abstracted polymer chains then reside on top of the initial-layer chains and form a second layer. On the completion of this layer, at a particular I, the process is repeated and polymer chains are assimilated into a third layer; 2) For a given I, all abstracted polymer chains have the same radius of gyration, $(r_G)_{ABS}$, irrespective of their placement in the abstracted layers. Therefore, the abstraction densities and the thicknesses of complete layers are equal at a given I; 3) $(r_G)_{ABS}$ decays with increasing I, and the form of this decay is taken to be that observed in the development of the initial layer and described by Eq. (13). Thus, more polyacrylate is accommodated in each of the innermost layers, and there is a steady rise in the abstraction density of these layers, as the dose (i.e. I) is increased; 4) For a given I, the volumes occupied by a polymer chain in the abstracted state and in bulk solution are equal[2].

Molecular footprint, molecular radius and abstraction density in the initial layer, in the region of multilayer formation (i.e. Region 3)

F_1 in the region of multilayer formation may be calculated by means of the relation

$$F_1 = \pi r_{ABS}^2 , \tag{14}$$

where

$$r_{ABS} = (r_G)_{ABS}(5/3)^{(1/2)} , \tag{15}$$

and $(r_G)_{ABS}$ is given by Eq. (13). Then, Γ_1 in the

[2] The shape of the volume occupied by a polymer chain in bulk solution is taken as spherical.

region of multilayer formation may be calculated from F_1 by means of the relation

$$\Gamma_1 = 10^{24}\,\mathrm{M}/(FN)\,, \tag{16}$$

with F equal to F_1.

Layer thickness

The inequality $(r_G)_{ABS} < (r_G)_{SOL}$ shown in Fig. 6, may be taken to infer a lateral compression of the abstracted (and collapsed) polymer chains. The simplest shape of laterally compressed polyacrylate chains in an abstracted layer, j, is a cylinder of radius r_{ABS} and height (or thickness) δ_j. In view of the assumed equivalence of volumes cited above, the thickness δ_j (in units of nm) of the abstracted polymer layer is given by

$$\delta_j = 4r_{SOL}^3/3r_{ABS}^2\,, \tag{17}$$

where r_{SOL} is the actual radius (in units of nm) of sodium polyacrylate in bulk solution, and is given by

$$r_{SOL} = (r_G)_{SOL}(5/3)^{(1/2)} \tag{18}$$

and $(r_G)_{SOL}$ is given by Eq. (12). The thickness of each abstracted layer was calculated in this way.

Abstraction density, molecular footprint and molecular radius in the second layer up to the completion of this layer

The amount of polyacrylate abstracted into the second layer may be obtained from the difference

$$\gamma_2 = \gamma_{TOT} - \gamma_1\,, \tag{19}$$

where γ_1 is the amount of polyacrylate abstracted into the first layer, and is given by

$$\gamma_1 = S\Gamma_j/1000\,, \tag{20}$$

with $S = 5.7\ \mathrm{m^2\,g^{-1}}$ and $\Gamma_j = \Gamma_1 . \gamma_2$ may be converted into an abstraction density (Γ_2) in the second layer using the relation

$$\Gamma_2 = 1000\gamma/S\,, \tag{21}$$

with $\gamma = \gamma_2$, and S = the geometric specific surface area (S_1) of the calcite with a single layer of abstracted polyacrylate (i.e. the geometric specific surface area at the outer edge of the first abstracted layer): S_1 is given by Eq. (1) with $r = R + \delta_1$.

The average molecular footprint (F_2) of polyacrylate in the second layer is given by Eq. (9) with $\Gamma_j = \Gamma_2$. The actual radius of this footprint is given by Eq. (10) with $F = F_2$, while the equivalent radius of gyration is obtained using Eq. (11).

Abstraction density, molecular footprint and molecular radius in the second layer, in the region of layer three formation

The second layer was considered to be complete when its abstraction density became equivalent to that of the first layer. This occurred at $\Gamma_2 \approx 448\ \mu\mathrm{g\,m^{-2}}$ and a dose of ca. 16.0 mg per g. Thus, the second layer was complete at the two highest doses, viz., 19.7 and 27.9 mg per g.

The F_2, r_{ABS} and Γ_2 of polymer chains in the second layer at the two highest doses, i.e. in the region of layer 3 formation, are given, respectively, by Eqs. (14), (15) and (16) with $F = F_2$.

The abstraction density, molecular footprint and molecular radius in higher layers (i.e. third and fourth layers) may be calculated in an analogous manner to that described above for the first two layers.

The variation of the total layer thickness (δ_{TOT}, equal to $\delta_1 + \delta_2 + \delta_3 + \delta_4$) with dose is shown in

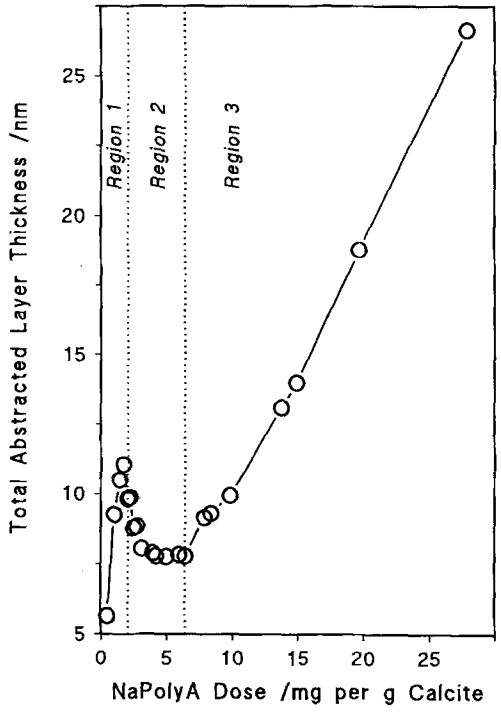

Fig. 9. Total abstracted layer thickness as a function of NaPolyA dose

Table 2. Characteristics of the layers of polyacrylate abstracted by a calcite surface

Layer	Dose at completion of layer	Ionic strength at completion of layer	Abstraction density of a complete layer at this ionic strength	Thickness of a complete layer at this ionic strength
	mg per g Calcite		$\mu g\,m^{-2}$	nm
1	6.4	0.139	366	7.76
2	16.0	0.318	448	7.38
3	23.2	0.447	470	7.30

Fig. 9, while the characteristics of the layers of abstracted polyacrylate are given in Table 2.

Thus, the model predicts a sharp increase in δ_{TOT} with dose in Region 1. This correlates well with the sharp uptake of cation polyacrylate in this region, as quantified in Fig. 3. It may be inferred, therefore, that polyacrylate uptake is more important than chain collapse in Region 1. δ_{TOT} attains a value of ca. 9.8 nm at a dose of ca. 2 mg per g.

In Region 2, the model predicts a sharp decrease in δ_{TOT} after which δ_{TOT} remains fairly steady at a value of ca. 7.8 nm up to a dose of ca. 6 mg per g. Such a reduction in δ_{TOT} with increase in I (i.e. increase in dose) has been observed by several groups [15, 16, 25, 26]. It may be inferred, therefore, that chain collapse dominates polymer uptake in Region 2.

In Region 3 the model predicts a steady increase in δ_{TOT} with increase in I (i.e. increase in dose). This correlates well with the multilayer uptake of polyacrylate in this region as quantified in Fig. 3. It may be inferred, therefore, that polyacrylate uptake dominates chain collapse in Region 3.

Particle–particle interactions, incorporating a steric energy term

An additional potential energy term (V_S) was introduced into the calculation of V_T to provide a measure of the steric repulsion between abstracted polyacrylate chains residing on approaching calcite particles. Thus, V_T was now calculated from the summation ($V_R + V_A + V_S$). The equation of Ottewill [23] was used to describe the variation of V_S with h:

$$V_S = 4\times10^{-27}\pi C^2 kT\cdot(\psi - \chi_2)(\delta_{TOT} - h/2)^2 \times(3R + 2\delta_{TOT} + h/2)/3vp_2^2\,, \quad (22)$$

where C is the concentration (in units of $mg\,cm^{-3}$) of cation polyacrylate in the total layer of abstracted polyacrylate, v is the molecular volume of water molecules ($18.02\times10^{-6}/N\,m^3$), p_2 is the density of the abstracted polyacrylate ($1300\,mg\,cm^{-3}$), ψ is a dimensionless entropy parameter, which for ideal mixing can be taken as 0.5, and χ_2 is the dimensionless NaPolyA/solution interaction, or solvency, parameter. C is given by the expression

$$C = \Gamma^1_{TOT}/\delta_{TOT}\,, \quad (23)$$

where $\Gamma^1_{TOT} = (\Gamma_1 + \Gamma_2 + \Gamma_3 + \Gamma_4)$. C rose sharply with dose in Regions 1 and 2, and then tended toward a limiting value of ca. $65\,mg\,cm^{-3}$ in Region 3; the variation of C with dose was described very well by an asymmetric sigmoid function. The variation of χ_2 with I, for sodium polyacrylate, has been evaluated by Rogan [17], from the intrinsic viscosity data of Takahashi [18]. The variation is expressed as the linear function

$$\chi_2 = -0.02167/I^{1/2} + 0.5232 \quad (24)$$

The variation of V_T, scaled in units of kT, with h (interaction energy curve) is shown in the three plots (corresponding to the three dose-range regions) of Fig. 10. The behaviour of the ($V_R + V_A + V_S$) interaction energy curves with increasing dose is similar to that of the ($V_R + V_A$) curves (shown in Fig. 8) up to a dose of ca. 6 mg per g, i.e. just prior to multilayer formation at the end of Region 2. However, at higher doses (i.e. in Region 3) the behaviour of the two sets of curves differ, in that the heights of the energy curves computed with a steric repulsive term increase steadily with dose, above a dose of ca. 6 mg per g. Thus, the formation of multiple layers of polyacrylate on the calcite surface gives rise to a strong steric repulsion which dominates interparticle interactions.

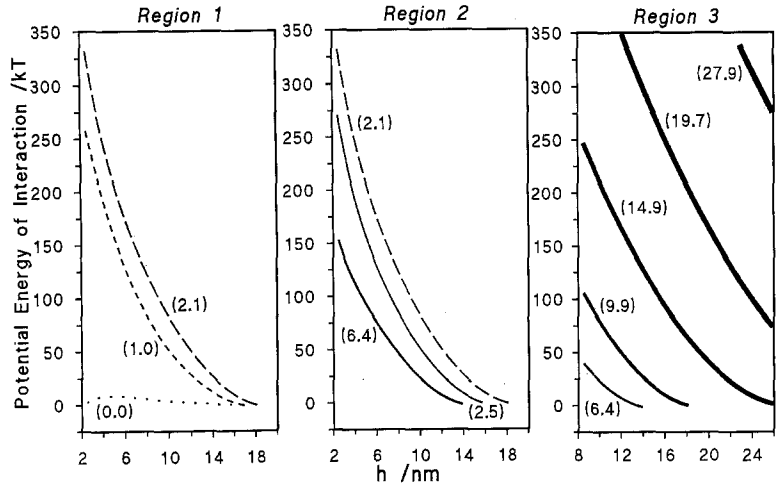

Fig. 10. Interaction energy curves: van der Waals attraction + electrostatic repulsion + steric repulsion. Values in parentheses are NaPolyA dose in units of mg per g calcite

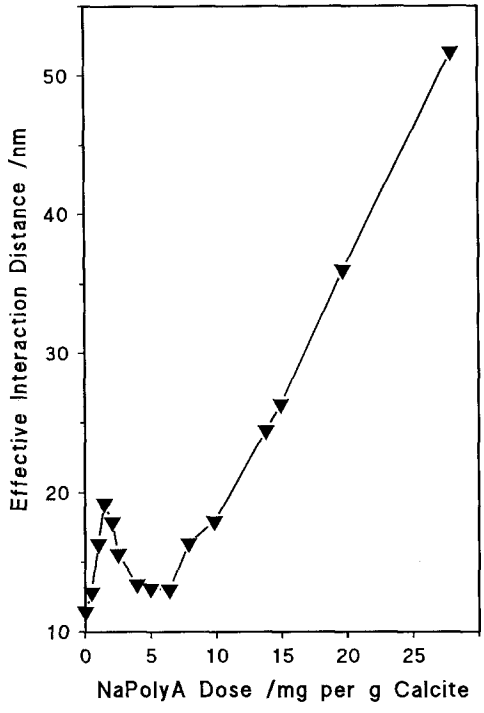

Fig. 11. Effective interaction distance as a function of NaPolyA dose

This occurs in a high I region in which electrostatic repulsion is negligible.

Inter-particle interaction distance

A useful way of describing particle-particle interactions is to calculate the effective surface to surface interaction distance (H, in units of nm). Following Ottewill and Richardson [27], this can be done by utilising the theory of Barker and Henderson [28, 29]. Using their approach H is defined as

$$H = \int_0^\infty [1 - \exp(-V_T/kT)]dh \qquad (25)$$

The function $[1 - \exp(-V_T/kT)]$ decayed sharply with increase in h, for all but the very lowest doses (i.e. 0 and 0.49 mg per g) indicating that the particles interact to a first approximation as hard spheres, for most of the dose range covered. The computed H values are plotted against dose in Fig. 11. H is about 15 nm throughout Regions 1 and 2, and then rises steadily to ca. 50 nm in Region 3. It is of interest to compare the H values with the estimated surface-to-surface distance (H_{LAT}, in units of nm) between particles based on a concept of a f.c.c. lattice. H_{LAT} was obtained using the expression

$$H_{LAT} = R[(1.8094\phi^{(-1/3)}) - 2]\ ; \qquad (26)$$

this gave the value of 65.5 nm for H_{LAT}. That is, $H < H_{LAT}$ over the dose range studied. Thus, the interactions between calcite particles at a slurry solids of 70% ($\phi = 0.463$) are such that the system is not highly ordered but the particles are apparently arranged in a "liquid-like" configuration. However, on the assumption of a f.c.c. packing of particles, it is envisaged that the system will attain a "glass-like" state at a dose of ca. > 30 mg per g.

Conclusions

Sodium polyacrylate has a high affinity for a calcite surface and a monolayer is assimilated at low doses, ca. 2 mg per g. Hardly any polyacrylate remains in the continuous phase and the I of this medium is low and increases only slightly with dose. The polymer chains are in a relatively extended configuration and the thickness of the monolayer is modelled to be ca. 9.8 nm. In this low I region, the electrical double layers of particles are relatively extensive. As a result, the initial uptake of polyacrylate (anionic polyelectrolyte) generates quite high, negative zeta potentials, ca. -45 mV. In such a situation of extensive double layers and high zeta potentials, the electrostatic repulsion between approaching particles is strong and a slurry of the particles is colloidally stable.

The colloidal stability of slurries of the polyacrylate-covered particles is evident from the sharp fall in slurry viscosity observed at low levels of sodium polyacrylate addition.

With further addition, more and more polyacrylate appears in the continuous phase and a steady increase in I is observed with increase in dose; the main contributors to I are sodium cations and polyacrylate anions.

The sodium polyacrylate exchanges Na^+ ions for Ca^{2+} and Mg^{2+} ions, and water-soluble, mixed polyacrylates (eg. sodium-calcium-polyacrylate) are produced. With the uptake of virtually all the polyacrylate at low doses, this exchange results in the Ca^{2+}/Mg^{2+} depletion of the continuous phase as these ions are taken to the calcite surface. However, as more polyacrylate appears in the continuous phase at higher doses, this exchange now gives rise to increasing concentrations of these cations as the polyacrylate exchanges Na^+ ions for solid phase Ca^{2+}/Mg^{2+} ions.

The steady increase in I leads to a collapse of surface polyacrylate chains and the production of vacant surface onto which further polyacrylate then binds. However, the rate of production of vacant surface cannot keep pace with the rate of uptake of polyacrylate chains, and multilayer formation begins at a dose of ca. 6 mg per g. The thickness of the initial layer, at this stage is modelled to be ca. 7.8 nm. The increase in I also collapses electrical double layers and this effect begins to dominate over the observed increase in zeta potential arising from the uptake of polyacrylate. In terms of DLVO theory, interparticle electrostatic repulsion begins to diminish with increasing dose above ca. 2 mg per g.

Zeta potential attains a maximum value just prior to the onset of multilayer formation, and is then increasingly suppressed by the steady rise in I throughout multilayer assimilation.

In spite of the predicted diminution in electrostatic repulsion, the viscosities of slurries of polyacrylate covered particles continue to decay with dose up to and beyond 6 mg per g. On the reasonable assumption that such a decay in viscosity infers an increase in colloid stability, then such stability cannot be explained solely on the basis of electrostatics. Apparently, the notion that the colloidal stability of sodium polyacrylate-treated calcite slurries is due entirely to the development of electrostatic repulsion between particles, is an inadequate representation of the true picture above a dose of ca. 2 mg per g.

The formulation of a model to characterise the uptake of multiple layers of polyacrylate, based on the observed collapse of polyelectrolyte chains with increasing I, leads to the evaluation of second and third layer completions at doses of ca. 16.0 and 23.2 mg per g, respectively. Using this model, the layer thicknesses at these doses were calculated to be ca. 7.4 and 7.3 nm, respectively.

The characterisation of abstracted polyacrylate multilayers by this model enables an assessment to be made of the steric repulsive energy between polyacrylate-covered particles. Calculations have shown that the incorporation of such a repulsion in the total interparticle interaction energy can generate increasing colloidal stability above ca. 6 mg per g and so reconcile theory with experiment. It would appear that, while electrostatic repulsion diminishes, steric repulsion increases with dose. Thus, in the dose range ca. 2 to 6 mg per g, colloidal stability is a result of both electrostatic and steric repulsions (i.e. electrosteric repulsion). In contrast, above ca. 6 mg per g, stability is achieved almost solely by steric repulsion, while electrostatic repulsion in this high I region is negligible.

Although the colloid particles increase in size with dose as polyacrylate layers are built up, the viscosity of a slurry of the particles continues to decay even at high doses (i.e. up to ca. 28 mg per g)

because the colloid particles are still small enough to be freely mobile, and thereby allow the inter-particle steric repulsion to operate. However, it is envisaged that the colloid particles will touch, and the system will attain a "glass-like" state, at a dose of ca. > 30 mg per g.

Acknowledgements

The authors are indebted to Professor R.H. Ottewill, Professor B. Vincent, Professor B.R. Jennings, J.C. Husband, C.R.L. Golley and J.A. Purdey for valuable discussions, to Dr. N.J. Elton for computational assistance, and to G.W.A. Beard and D. Mogridge for technical assistance. The authors also wish to thank the directors of ECC International, Dr. R. Bown and R.W. Adams for permission to write and publish this work.

References

1. Fuerstenau MC, Palmer BR (1976) In: Fuerstenau MC (ed) Flotation. AIME, New York, pp 151–152
2. Giesekke EW, Harris PJ (1984) Int Conf Miner Processing Johannesburg
3. Fuerstenau MC, Miller JD (1967) Trans AIME 238:153
4. Somasundaran P (1969) J Colloid Interface Sci 31:557
5. Han KN, Healy TW, Fuerstenau DW (1973) J Colloid Interface Sci 44:407
6. Rogan KR (1994) Colloid Polym Sci 272:82
7. Aplan FF, Fuerstenau DW (1962) In: Fuerstenau DW (ed) Froth Flotation. AIME, New York
8. Giles CH, MacEwan TH, Nakhwa SN, Smith D (1960) J Chem Soc p 3973
9. Giles CH, MacEwan TH (1957) Proc 2nd Int Conf Surf Activity 2:339
10. Corner T (1983) In: Poehlein GW, Ottewill RH, Goodwin JW (eds) Science and technology of polymer colloids NATO ASI series E, Martinus Nijhoff, The Hague, pp 600–618
11. Munk P (1989) Introduction to macromolecular science, Wiley-Interscience, New York, pp 59–61
12. Cohen-Stuart MA, Cosgrove T, Vincent B (1986) Adv Colloid Interface Sci 24:143
13. Bonekamp BC, van der Schee HA, Lyklema J (1983) Croat Chem Acta 56:695
14. Cafe MC, Robb ID (1982) J Colloid Interface Sci 99:341
15. Takahashi A, Kawaguchi M, Kato T (1980) In: Lee L-H (ed) Adhesion and adsorption of polymers polymer science and technology volume 12b, Plenum, New York, pp 729–749
16. Takahashi A, Kawaguchi M, Hayashi K, Kato T (1984) In: Goddard ED, Vincent B (eds) Polymer adsorption and dispersion stability, ACS Symp Ser 240, pp 39–52
17. Rogan KR (1994) Colloid Polym Sci (submitted for publication)
18. Takahashi A, Nagasawa M (1964) J Am Chem Soc 86:543
19. O'Brien RW, White LR (1978) J Chem Soc Faraday Trans II 74:1607
20. White LR, Mangelsdorf C, Chan YC (1989) University of Melbourne
21. Derjaguin BV, Landau L (1941) Acta Physiochim, URSS 14:633
22. Verwey EJW, Overbeek JThG (1948) In: Theory of the stability of lyophobic colloids, Elsevier, Amsterdam, pp 160–163
23. Ottewill RH (1990) In: Candau F, Ottewill RH (eds) Scientific methods for the study of polymer colloids and their applications NATO ASI Series, Kluwer Academic, Dordrecht, pp 129–157
24. Hough DB, White LR (1980) Adv Colloid Interface Sci 32:205
25. Varoqui R, Derjardin Ph, Pefferkorn E (1978) J Colloid Interface Sci 63:353
26. Gramain Ph, Myard Ph (1981) J Colloid Interface Sci 84:114
27. Ottewill RH, Richardson RA (1982) Colloid Polym Sci 260:708
28. Barker JA, Henderson D (1967) J Chem Phys 47:4714
29. Barker JA, Henderson D (1972) Ann Rev Phys Chem 23:439

Received November 18, 1993;
accepted April 29, 1994

Authors' address:

Dr. Keith R. Rogan
Research Department
ECC International
John Keay House
St. Austell, United Kingdom